

Growth of Nd³⁺ doped LiNbO₃ crystals using Bridgman method and its spectral properties

JINHAO WANG^{*,†,††}, YUEPING ZHANG[†], HAIPING XIA[†] and JIAWEI SHENG^{††}

[†]Laboratory of Photo-Electronic Materials, Ningbo University, Ningbo 315211, PR China

^{††}College of Chemical and Materials Engineering, Zhejiang University of Technology, Hangzhou 310014, PR China

MS received 23 July 2008; revised 10 October 2008

Abstract. The growth of Nd³⁺ doped lithium niobate crystals using Bridgman method has been reported in this paper. By means of the optimum conditions such as proper feed materials, sealed platinum crucibles, growth rate of 1–1.5 mm/h and temperature gradient of 30–35°C/cm across the solid–liquid interface under the furnace temperature of 1300°C, single crystals containing Nd³⁺ ion with 0.54 mol% concentration were obtained. X-ray diffraction and ICP–AES were used to characterize the crystals and its composition. The absorption, emission and fluorescence lifetime are also measured. Based on the Judd–Ofelt theory, we obtained the optical parameters of the crystal such as the luminescent quantum efficiency, the radioactive lifetimes, the branching ratios and the emission cross-section.

Keywords. Nd³⁺-doped LiNbO₃; crystal growth; spectral properties; Bridgman method.

1. Introduction

Lithium niobate is well known as a multi-functional crystal, which has been extensively used in solid-state lasers, opto-electronic devices and high resolution holographic storage due to its excellent property (Johnson Ballman 1969; Armenise *et al* 1983; Bordui *et al* 1992). Doping with foreign ions modifies the optical properties of the matrix and makes the crystal useful for a great variety of application like Nd³⁺ doped LiNbO₃ crystals, which has been applied for the compact diode-pumped self-frequency-doubled lasers which contain much potential in high optical data storage, undersea imaging, diagnosis in medicine, excitation sources to replace ion gas lasers for science and pumping of parametric oscillators and amplifiers (Capmany *et al* 1999).

It is known to all that the congruent LiNbO₃ presents a low threshold for photorefractive damage because of Li deficiency. Although, adding a small amount of MgO or ZnO would improve the photorefractive damage threshold (Bryan *et al* 1984; Volk *et al* 1990), but co-doping with impurities would somewhat bring about other problems, such as reduced optical quality, dark trace induced by the high power laser beam in Mg-doped LiNbO₃ and difficulty of the growth (Jaque *et al* 2000). It has been realized that the stoichiometric LiNbO₃ crystal or less amount of MgO or ZnO doped stoichiometric LiNbO₃

crystal is emerging as an alternative to congruent LiNbO₃ crystal. The stoichiometric LiNbO₃ crystal was used to produce by double crucible Czochralski method with automatic powder feeding technique (Kitamura *et al* 1992), vapour transport equilibration technique (Solanki *et al* 2003), top seeded solution growth technique with K₂O as flux (Bordui *et al* 1992), zone leveling technique (Tsai *et al* 2006), and top seeded solution growth technique with 58 mol% Li₂O composition (Babu Reddy *et al* 2008). In this paper, we tried to grow Nd³⁺-doped stoichiometric LiNbO₃ crystals by Bridgman method with superfluous Li₂O composition, using sealed platinum crucible and a small temperature gradient to prevent Li₂O from evaporating.

2. Experimental

The feed material for LiNbO₃ crystal growth was synthesized with high purity Li₂CO₃ (4N purity) and Nb₂O₅ (4N purity), and the molar ratio of Li₂O to Nb₂O₅ was adopted as about 1.08. Too much Li₂O would make the crystallization of crystal difficult and the transparent part would also be reduced. The mixture was sintered at a temperature of 1180°C in a furnace. Nd₂O₃ (4N purity) was mixed into the polycrystalline powder with 0.5 mol% concentration as the initial dopants.

The equipment of crystal growth is mainly composed of furnace, temperature control panel and pulling down mechanism, which is shown in figure 1. Pt–Pt/Rh 10% thermocouples located at the upper part of furnace and

*Author for correspondence (cxycwjh@yahoo.com)

around the seed were used to detect the temperature. The furnace temperature was adjusted by a TCW-32B fine temperature controller with an accuracy of $\pm 0.5^\circ\text{C}$ during the whole process. The crystal was grown in a two-zone resistively heated furnace. The temperature of the melting zone was usually controlled at $1290\sim 1300^\circ\text{C}$, which was $70\sim 80^\circ\text{C}$ higher than the melting point of crystal. The platinum crucible used in crystal growth was 24 mm in diameter and 200 mm in length. Put a seed which was 10 mm in diameter at the bottom of platinum crucible, and sealed up the top of platinum crucible after charged with 150 g feed materials. The platinum crucible was installed in a refractory tube filled with Al_2O_3 powder in order to reduce the temperature fluctuations. The refractory tube together with the crucible was moved into the furnace chamber. After the furnace had been heated to controlled temperature, the crucible was then adjusted to a position where only the top of the seed was melted. The feed material and the top of the seed were kept at the melting state for several hours so that a stable solid-liquid interface could be established on the top region of the seed, and then the crucible was pulled down at a rate of $< 2\text{ mm/h}$. The temperature gradient across solid-liquid interface was $30\sim 40^\circ\text{C/cm}$. The whole process of crystal growth would hold for about one week. After the growth had finished, the furnace was cooled slowly to room temperature and the crystal was obtained by stripping the platinum crucible. The crystal was cut and polished to 1.5 mm thick wafer from the transparent part for spectral measurements.

The crystalline phase of $\text{Nd}^{3+}:\text{LiNbO}_3$ was identified by powder X-ray diffractometer (XD-3, Purkinje) equipped

with $\text{CuK}\alpha$ radiation ($\lambda = 1.5406\text{ \AA}$). The composition of the crystal and the concentration of Nd^{3+} were measured by inductively coupled plasma-atomic emission spectrometry (ICP-AES). The optical absorption spectra were measured using a Perkin-Elmer Lambda 900UV-Vis-NIR spectrometer, and the fluorescence spectrum was measured by Hitachi F4500 fluorescence spectrometer at room temperature.

3. Results and discussion

3.1 Characterization of crystal

The obtained $\text{Nd}:\text{LiNbO}_3$ crystal has a diameter of 24 mm as shown in figure 2. The crystal is mostly transparent, and there is some white aggregation and cracking on the tail part of the crystal because of incongruent of composition. Figure 3 shows the X-ray diffraction patterns



Figure 2. $\text{Nd}:\text{LiNbO}_3$ crystal grown by the Bridgman method.

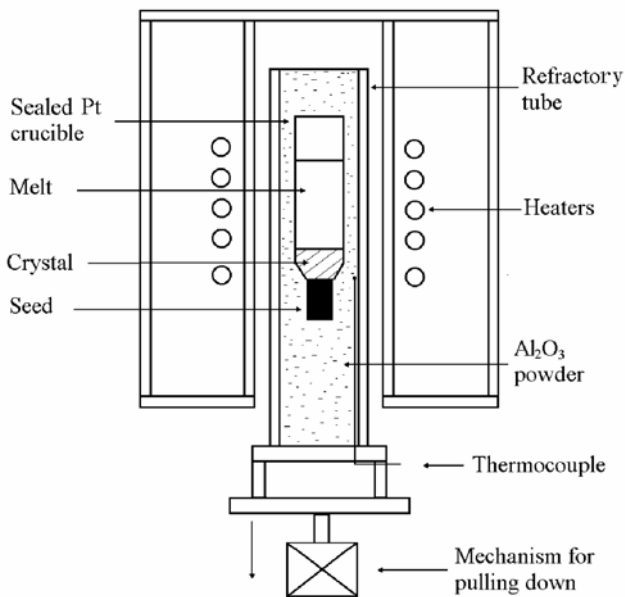


Figure 1. Scheme diagram of the Bridgman furnace of crystal growth.

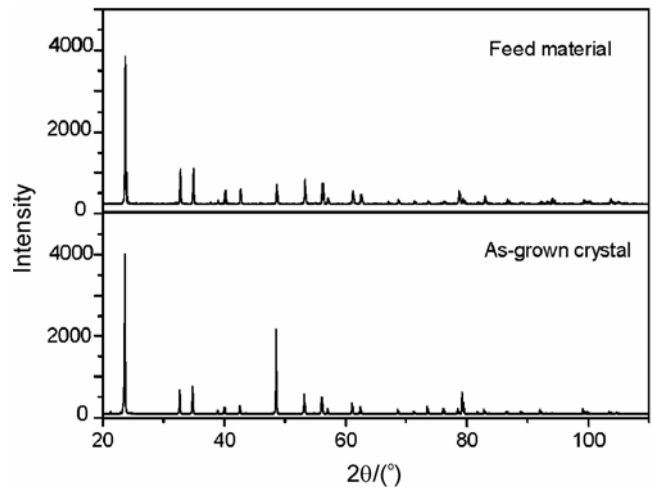


Figure 3. XRD curves of the feed material and the as-grown $\text{Nd}:\text{LiNbO}_3$ crystal.

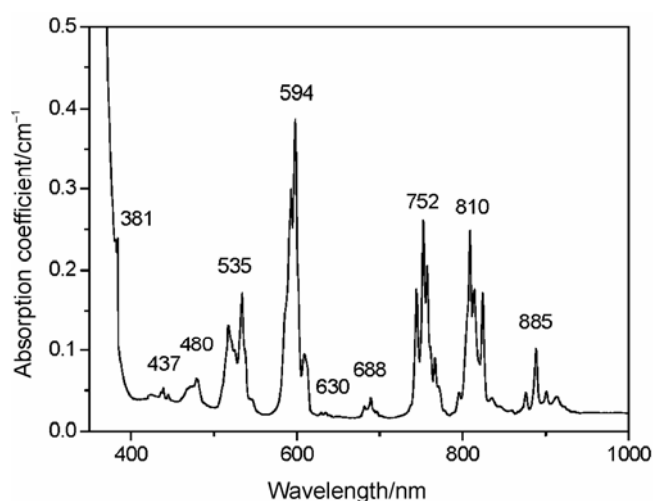
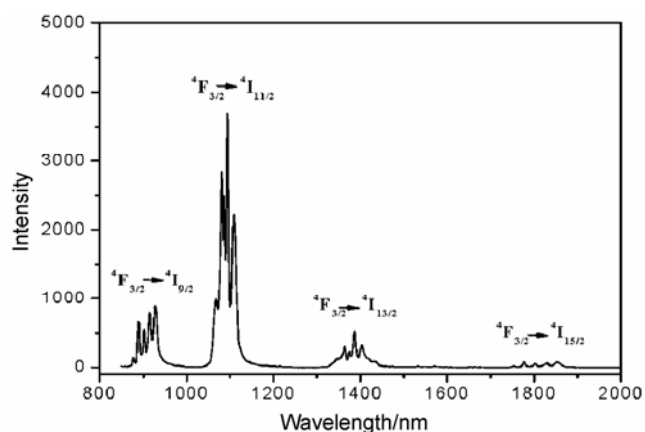
Table 1. The concentration of the feed material and the obtained crystals.

Sample	Li (mol%)	Nb (mol%)	Li : Nd ratio	Nd (mol%)
Feed material	51.75	47.75	1.08	0.5
Obtained crystal	49.1	50.36	0.97	0.54

Table 2. Calculated Judd–Ofelt parameters of Nd^{3+} ions in the LiNbO_3 crystal.

Levels	Wavelength (nm)	A_r (s^{-1})	β	$\sigma_{\text{em}}^{\text{calc}}$ ($\times 10^{-20} \text{ cm}^2$)	$T_r = 1/W_R$ (μs)	T_{exp} (μs)	η
${}^4F_{3/2}$					436	240	0.55
${}^4I_{9/2}$	907	897.0	0.39	0.27			
${}^4I_{11/2}$	1096	1189.3	0.52	1.02			
${}^4I_{13/2}$	1386	198.1	0.08	0.22			
${}^4I_{15/2}$	1800	9.8	0.01	0.02			

$\Omega_2 = 4.05$, $\Omega_4 = 2.71$, $\Omega_6 = 4.27 (\times 10^{-20} \text{ cm}^2)$

**Figure 4.** The absorption spectrum of the Nd : LiNbO_3 crystal.**Figure 5.** The fluorescence spectrum of the Nd : LiNbO_3 crystal.

of feed materials and the obtained crystal. By comparing with the JCPDS card of lithium niobate (No: 20-0631), it is confirmed that the obtained crystal is a single phase of LiNbO_3 . The feed material also is LiNbO_3 phase but contained less extra Li_2O or other lithium niobate phases.

The concentrations of Li, Nb, Nd ions in the feed material and the obtained crystal are all listed in table 1.

Compared with the Czochralski process, the volatilization of Li_2O can be avoided effectively by sealing the crucible in our Bridgman process, the composition of melts could be kept stable in order to grow high quality crystals (Chen *et al* 2003). The Li/Nb ratio being close to stoichiometric resulting from ICP–AES measurement enhanced this issue.

3.2 Optical properties of Nd : LN

Samples were cut out of boluses and the surface perpendicular to the $\langle 001 \rangle$ -growth axis was polished for the spectroscopic measurements. Absorption spectra were measured at room temperature in the wavelength range from 300–1100 nm. The thickness of the samples is 1.5 mm.

The absorption spectra of as-grown Nd : LN are shown in figure 4 where exists ten well distinguished groups of bands characteristic for transitions from the ${}^4I_{9/2}$ ground state to the excited states. The bands around 810 nm wavelength region corresponding to the ${}^4I_{9/2} \rightarrow {}^4F_{3/2} + {}^2H_{9/2}$ transition have relatively higher absorption and broad FWHM of 23 nm which is easy for commercial diode laser pumping.

We achieved pumping of the ${}^3F_{3/2}$ level using an 807 nm diode laser pump in room temperature, which is shown in figure 5. Aside from the ordinary infrared emission around 927 nm, 1100 nm and 1400 nm responding to the ${}^3F_{3/2} \rightarrow {}^4I_J$ ($J = 9/2, 11/2, 13/2$) transitions, we also observed the emission around the bands of 1800 nm, which attribute to the ${}^3F_{3/2} \rightarrow {}^4I_{15/2}$ level transition.

The radiative properties of Nd^{3+} ions in the LiNbO_3 crystal were described by the Judd–Ofelt theory (Judd 1962; Ofelt 1962). The reduced matrix elements of tensor operators $U^{(t)}$ was obtained from Carnall *et al* (1968). The calculated phenomenological intensity parameters (Ω_λ), radiative transition rates (A_r), total radiative lifetimes (T_r), and the branching ratios (β) are listed in table 2.

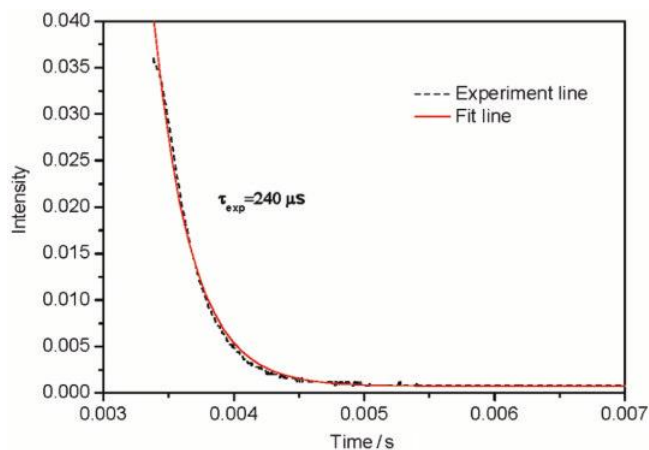


Figure 6. The fluorescence decay curve and fitting curve of the ${}^4F_{3/2}$ level of Nd^{3+} in the LiNbO_3 crystal.

For lines with Lorentz line shape, the stimulated emission cross-section, σ_{em} , for the transition ${}^3F_{3/2} \rightarrow {}^4I_J$ ($J = 9/2, 11/2, 13/2, 15/2$) was estimated using the formula (Huber *et al* 1975)

$$\sigma_{\text{em}} = \frac{A_i \lambda_p^2}{4\pi^2 n^2 c \Delta\nu}, \quad (1)$$

in which λ_p is the wavelength of the fluorescent peak, n the refractive index, c the speed of light and $\Delta\nu$ the frequency of full width at half-maximum. The result has been shown in table 2. Resulting from calculation, the most important transition ${}^3F_{3/2} \rightarrow {}^4I_{11/2}$ has the maximal branching ratio and emission cross-section which is 52% and $1.02 \times 10^{-20} \text{ cm}^2$, respectively.

The measured fluorescence lifetime decay curve of the ${}^3F_{3/2}$ levels is shown in figure 6 and the fitted lifetime, τ_{exp} is 240 μs . As the calculated irradiative lifetime, τ_r , is 436 μs , so the luminescent quantum efficiency of the ${}^3F_{3/2}$ levels is about 55%.

4. Conclusions

The Nd^{3+} doped LiNbO_3 single crystals were obtained by using the Bridgman method. The crystal was of good optical quality by means of some optimum conditions. The absorption and luminescence spectra of crystal were

measured at room temperature. The crystal has a broad FWHM of 23 nm at 810 nm which is suitable for commercial diode laser pumping. Resulting from the Judd–Ofelt theory, the luminescent quantum efficiency of ${}^3F_{3/2}$ is 55%, the most important transition ${}^3F_{3/2} \rightarrow {}^4I_{11/2}$ which is of 1096 nm has the maximal fluorescent ratio, β , of 52% and the emission cross-section, σ_{em} , of $1.02 \times 10^{-20} \text{ cm}^2$. We are now working on enhancing of laser efficiency relying on the growth of near-stoichiometry crystal by fluxed-Bridgman method.

Acknowledgements

This work was supported by K C Wong Magna Fund in Ningbo University and Foundation of Ningbo University (No: xk2006).

References

- Armenise M N, Canali C, De Sario M and Zanoni E 1983 *Mater. Chem. Phys.* **9** 267
- Babu Reddy J N, Ganesh Kamath K and Vanishri S 2008 *J. Chem. Phys.* **128** 244709
- Bordui P F, Norwood R G and Jundt D H 1992 *J. Appl. Phys.* **71** 875
- Bryan D A, Gerson R and Tomaschke H E 1984 *Appl. Phys. Lett.* **44** 847
- Capmany J, Jaque D, Sanz Garcia J A and García Solé J 1999 *Opt. Commun.* **161** 253
- Carnall W T, Fields P R and Rajnak K 1968 *J. Chem. Phys.* **49** 4424
- Chen H B, Xia H P and Wang J H 2003 *J. Cryst. Growth* **256** 219
- Huber G, Krühler W W, Bludau W and Daniemeyer H G 1975 *J. Appl. Phys.* **46** 3580
- Jaque D, Capmany J and García Solé J 2000 *Appl. Phys.* **B70** 11
- Johnson L F and Ballman A A 1969 *J. Appl. Phys.* **40** 297
- Judd B R 1962 *Phys. Rev.* **127** 750
- Kitamura K, Yamamoto J K and Iyi N 1992 *J. Cryst. Growth* **116** 327
- Ofelt G R 1962 *J. Chem. Phys.* **37** 511
- Solanki S, Chong T and Xu X 2003 *J. Cryst. Growth* **250** 134
- Tsai C B, Hsu W T and Shih M D 2006 *J. Cryst. Growth* **289** 145
- Volk T R, Pryalkin V I and Rubinina N M 1990 *Opt. Lett.* **15** 996